INVESTIGATION OF SUPPORT STRUCTURES FOR DIRECT METAL LASER SINTERING (DMLS) OF IN625 PARTS

Ö. Poyraz*, E. Yasa*, G. Akbulut*, A.Orhangül*, S. Pilatin*

* TUSAS Engine Industries, Inc. Eskişehir, Turkey
REVIEWED

Abstract

Along with the increased application of additive manufacturing (AM) in the aerospace industry, a better understanding of different aspects for the technique has become necessary to fulfill the high demands of reliability and robustness. The ability to introduce very complex, even internal, features into part design with AM appeals everyday many design engineers to this new group of technologies. In this respect, new design rules for AM are being researched, developed and updated day-to-day. Although, it is commonly stated that AM offers limitless geometrical complexity, there are some limits of the technology. For Direct Metal Laser Sintering (DMLS), a metal powder fusion AM process, one of the major limitations in the geometrical freedom offered by AM is the overhang surfaces which necessitates melting on loose powder and lead to dross formation, distortions, curling, etc. Support structures to be built together with the target part thus become necessary and critical to avoid such undesired results and moreover to facilitate a uniform heat dissipation. Design of the support structures which are easy to apply and remove is therefore among the important research topics in AM. The compromise in the design of support structures roots from the fact that the support structures must be strong enough to connect the part to provide resistance for curling up and they are desired to be loose enough to be easily removed. In addition, redundant use of support structures increases the amount of material spent, production time as well as post-processing efforts. This paper presents an investigation of different support structure designs; applied onto a thin-walled IN625 part, manufactured using DMLS.

Introduction

According to ASTM F2792.429494-1 standard, additive manufacturing is the process of joining materials to make objects from 3D model data usually layer upon layer, as opposed to subtractive manufacturing methodologies, such as traditional machining [1]. Similarly, VDI 3404 standard defines AM as a manufacturing process in which the workpiece is built up in successive units or layers [2]. Laser Beam Melting (LBM), also referred to as direct metal laser sintering/melting (DMLS/DMLM), Laser Cusing® or Selective Laser Melting® (SLM) by different machine vendors or users, is a powder-based fusion process whereby a 3D part is produced, layer by layer, utilizing a high-energy focused laser beam to selectively melt powdered material and fuse the powder particles during solidification as defined in VDI 3404 [3]. One of the principal advantages of DMLS like other additive manufacturing techniques over conventional subtractive or formative methods does not come from the manufacturing approach, but from the geometrical complexity which is possibly to be added in the design of the part at almost no cost. [4]. The geometric complexity, which they offer, coupled with the freedom of tool-less manufacturing is compelling; however in practice, complete geometrical freedom is desired but not possible in complex overhanging geometries [5]. An overhang

zone corresponds to a downfacing part surface where powder has to be melted on top of loose powder particles instead of an earlier solidified part (see Figure 1 [6]). The melt pool created during scanning rests on loose powder rather than on solid material [7]. Previous research showed that the poor thermal conductivity of powder material leads to higher temperatures in the overhang areas and in the associated higher residual stresses after final cooling [8]. These diverse effects can cause various quality problems such as curling, warping, distortion, undesired surface roughness and complete fabrication failure in certain cases. Moreover, as shown in Figure 1, bad surface quality due to unwanted dross formation is a drawback.
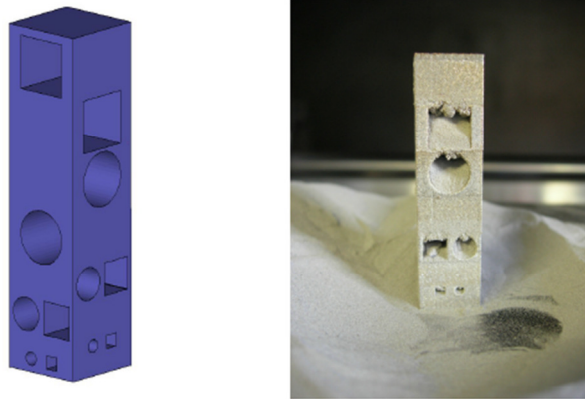

Figure 1: Overhang surfaces with different geometries and resulting dross formation [6]

Various measures can be taken to overcome the adverse effects of overhanging geometries, but these should be evaluated carefully. For instance, maintaining different part orientations is one of the measures that can be taken. However, proposed orientations should be optimized for more than one objective function, and these objective functions to optimize the part orientation selection in addition to eliminating overhang features are reducing stair effect and minimizing build time [9]. Besides, generally in complex geometries, there are more than one overhang surface which conflict each other regarding the optimized part orientation. Optimization of process parameters offer additional measures for overhanging surfaces, and parameters for optimization include spot diameter, laser power and scanning speed [8, 10, 11]. Still, they should be evaluated carefully, since these parameters have a direct effect on the build time. Although changing the scan speed in a very narrow region will not cause dramatic changes in the overall build time, the change of the process parameters shall be handled very carefully due to their direct effect on the porosity leading varying surface properties. Excluding the support structures for overhanging features, the final alternative as a measure is to carry out part designs according to design rules for additive manufacturing. These rules are assessed in both scientific [12, 13] and industrial works [14], providing a knowledge base for different types of processes, materials and geometries. In this regard, the need for information on new materials and processes remain, and research on the design rules is ongoing.

Supporting the overhanging geometries can be utilized alternatively or additionally to all of the above-described measures. These supports are used to prevent the object from toppling, or to support floating components and overhanging material [15]. Supports that are used for additive manufacturing can be found in two forms, which are similar material and secondary material supports. These structures are often massive and require additional post-processing time for their removal [16] which is also evident from the fact that the most common type of post-processing in additive manufacturing is support removal operations. In this respect,

secondary material supports present an effective way to remove from the part, such as in the case of Fused Deposition Modeling. By using secondary material supports, it is easy to distinguish support from part, to use a weaker material for support that can be removed easily or to apply a material that can be removed chemically without affecting the part [17]. However, for the powder-bed processes such as DMLS, supports have to be made using the same material as the part due to difficulties associated with using multiple materials such as mixing and recycling problems.

Initial research for single material supports has begun more than twenty years ago, mainly focusing on computational support generation techniques relevant to Stereolithography (SLA) [15] and Fused Deposition Modeling (FDM) [18]. One of the common objectives of these studies were to determine best build orientation, which requires minimum number of support structures for a given overhang angle threshold between 30-45 degrees. Other objectives included automation, speed of support generation and ease-of-use, which contributed to the development of CAD (Computer Aided Design) data preparation software for AM. In today's market, there are commercially available software capable of CAD data preparation for AM, and they are provided both as standalone packages [19-21] or embedded modules [22] running inside general purpose CAD software.

Current research activities about support structures are conducted in different fields but the main objective to reduce the amount of connection of support structures to the part remains similar with previous studies. In this context, some of the current research topics cover new support generation algorithms, experimental analysis on the support structures of basic geometric elements, modeling of support structures by means of finite element analysis and design of cellular support structures. The research on modeling the process and support structures has been performed in order to predict the effects of thermo-mechanical loads on the plastic deformation. Yet, there are other effects to be considered on the performance of support structures such as collapse and separation of overhanging geometries during the process. A list of example studies is provided in Table 1.

This study investigates the use of support structures for DMLS processing of Inconel 625 parts, which are used in aero-engines as a material for high temperature mechanical properties and also for resistance to oxidation, corrosion and pitting. This paper covers two set of experiments on support structures for an overhanging geometry parallel to XY plane rather than inclined surfaces, to be able to reflect the extreme conditions. Block supports are utilized for simplification and better understanding of the effects during experiments. A first set of experiments examine the impact of the support dimensions such as hatch distance of a block, while the second set of experiments focuses mainly on the effects of part-support contact in the form of teeth dimensions. Results of both experiments are controlled by means of dimensional inspection and light optical microscopy. Finally, conclusions have been extracted and trends are discussed.

Table 1- Example Research on Support Structures

Reference No	Subject / Scope	Part Material
[6]	Control of process parameters to improve surface quality by melt pool monitoring	Ti6Al4V
[11]	Control of process parameters to improve surface quality by melt pool monitoring	Ti6Al4V
[23]	Support structure algorithm	Applies to all
[24]	Design of cellular support structures	AISI 316L
[25]	Modeling of support structures by means of finite element analysis	AlSi12
[26]	Modeling of support structures by means of finite element analysis	AlSi12
[27]	Support structure algorithm	Applies to all
[28]	Support structure optimization algorithm	Applies to all
[5]	Design of cellular support structures	Ti6Al4V
[29]	Modeling of support structures by means of finite element analysis	AlSi12
[30]	Experimental analysis on the support structures	AlSi10Mg & Ti6Al4V

Experimental Procedure

In this study, a prismatic body with a parallel overhang is designed to create a simplified foundation for testing of different support structures. The so called prismatic body is 10 mm long, 10 mm wide and 15 mm tall with an overhang that is 10 mm long, 10 mm wide and 2 mm tall. The part design for experiments and the support related geometrical dimensions are given in Figure 2a.For the design of support structures Magics® [19] SG Module is used. Although SG Module for support generation provides the ability to generate different support types such point, line, block, web or contour, only the block type support structures are evaluated in the context of this study. Block type supports are preferred for volumetric parts and they contain hatches fragmented by a certain distance. Fragmenting supports into independent islands instead of uniting all, helps the removal of supports. However, both the hatch distance and fragmentation should be considered as design parameters. The illustration in Figure 2b provides the definitions for block support sections. Special designs can be utilized on the part-support interface to further facilitate the removal of support structures. In the scope of this research, tooth-like structures for connections of the supports to the part are used. These structures have a tapered width, starting wide at the top of the support surface and ending narrow at the bottom of the part surface for a constant height and a constant pitch. In some cases, the top of this tooth may enter the part itself to ensure a stronger joining between support and part layers. There are various terms for these dimensions such as base length, top length and tooth height. An illustration is provided in Figure 2c, to establish a clear understanding for the definitions of tooth dimensions.
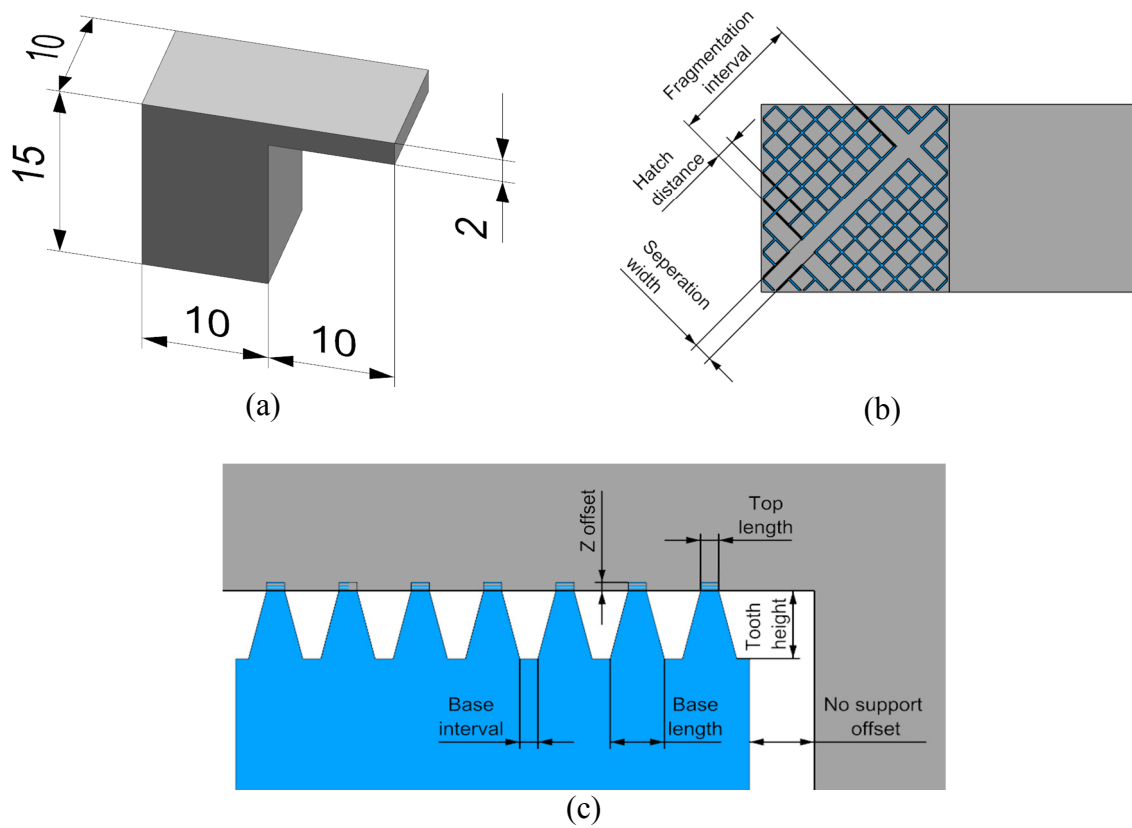
Figure 2: Designed part and dimensions for experiments (a), definitions for block supports (b), tooth dimensions (c)

In the first set of experiments, the effects of the hatch distance and fragmentation on the manufacturing results were investigated. The hatch distances were studied in three different levels as 0.5 mm, 0.75 mm and 1 mm, while the separation width always kept equal to hatch distance. Fragmentation interval was also considered as a factor of the hatch distance as 5, 6 and 7 times the length of hatch distance. For the mentioned experiments, a total of 9 samples were manufactured and controlled. In the second set of experiments, the influence of the top tooth length and Z offset on the manufacturing results were investigated. The top length values were studied in three different levels as 0.15 mm, 0.25 mm and 0.35 mm. Z offset values also have three levels as 0.040 mm, 0.120 mm and 0.200 mm, equivalent to 1 , 3 and 5 layers. For the second set of experiments, a total of 9 samples were manufactured and inspected. Table 2 shows design parameters for the 2 set of experiments. In the table, common parameters and factors with all levels are also presented for the 2 set of experiments. The figure from the CAD data preparation software is included in order to give an insight on the design matrix.

EOS Nickel Alloy IN625 was selected as the part material which has a wide application area in aero engine industry for different components such as engine exhaust systems, controls housing, turbine shroud rings and combustor liners. It has advantageous properties both for mechanical loads and chemical environment such as creep strength, rupture strength, thermal fatigue strength, oxidation resistance and corrosion resistance [31]. Table 3 shows the composition and as-built properties of the powder used in the experiments. The machine used

in experiments was EOS M290 and argon was utilized for protective atmosphere. One set of process parameters was used for all experiments only for examining the effect of geometric factors. These parameters are utilized for minimum porosity and different parameters are applied to different regions such as direct part, up skin, down skin, edges and external supports. These parameters together with a photo taken during laser scanning of test parts in the DMLS process are given in Table 4.

Table 2- Design parameters for experiment sets

1st Set of Experiments			2nd Set of Experiments		
Common parameters for all samples			Common parameters for all samples		
No support offset = 0.1 mm Tooth height = hatch distance Base length = hatch distance Top length = hatch distance / 2 Base interval = 0			No support offset = 0.1 mm Hatch distance = 0.5 mm Tooth height = hatch distance Base length = hatch distance Base interval = 0		
Sample no	Hatch distance (mm)	Fragmentation interval (mm) (x times hatch distance)	Sample no	Top length (mm)	Z offset (mm)
a-1	0.5	2.5 (x 5)	b-1	0.35	0.20
a-2	0.5	3.0 (x 6)	b-2	0.35	0.12
a-3	0.5	3.5 (x 7)	b-3	0.35	0.04
a-4	0.75	3.75 (x 5)	b-4	0.25	0.20
a-5	0.75	4.5 (x 6)	b-5	0.25	0.12
a-6	0.75	5.25 (x 7)	b-6	0.25	0.04
a-7	1	5 (x 5)	b-7	0.15	0.20
a-8	1	6 (x 6)	b-8	0.15	0.12
a-9	1	7 (x 7)	b-9	0.15	0.04
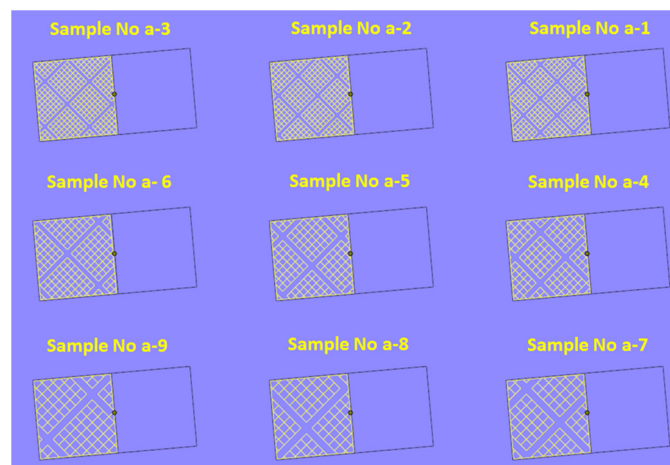
Table 3 – Properties of IN625 powder material [32]

Material Compositon											
Ni	Cr	Mo	NB	Fe	Ti	Al	Co	C	Ta	Si,Mn	P,S
balance	20 - 23 wt %	8 -10 wt %	3.1 - 4.1 wt %	≤ 5 wt %	≤ 0.4 wt %	≤ 0.4 wt %	≤ 0.1 wt %	≤ 0.1 wt %	≤ 0.05 wt %	≤ 0.5 wt %	≤ 0.01 wt %

As Built Properties at Room Temperature						
Direction	Density	Tensile Strength	Yield Strength	Modulus of Elasticity	Elongation at Break	Hardness
Horizontal (XY)	8.4 g/cm^3	990 MPa	725 MPa	170 GPa	35 %	30 HRC
Vertical (Z)	8.4 g/cm^3	900 MPa	615 MPa	140 GPa	42 %	30 HRC

Table 4 – Processing of parts

	Power	Speed	Layer thickness	Overlap
Part	285 W	960 mm/s	0.040 μm	0.080 mm
Supports	100 W	900 mm/s	0.040 μm	Single line

Evaluation of Results

After manufacturing, dimensional inspection and microstructural evaluations were carried out for the resultant parts in as-built condition. Dimensional inspection was conducted by a height gage in order to see the part distortions in the upward direction to check the effectiveness of the created supports. Since the parts were in as-built condition, the flatness of the base plate was measured first to avoid wrong interpretation of the results. For both set of experiments, flatness value of the plate was less than 4 μm. The heights of 4 points were measured on the top part surface. These points were referred with the letters a, b, c, d and measurement points "a" and "d" were located on the edge of overhanging surface while the points "b" and "c" were located on the edge of part surface. Point graphs were generated by using measurement results for each sample to provide better interpretation options. However, the 7th, 8th and 9th sample of the first set were not measured since there was a visible separation of supports from the parts, which can be seen clearly in the part photos.

Illustration of measurement routine, resulting part photos and line graphs are given within Table 5.

Initially, a correct interpretation of results is required for increased distortion and separation observed on the specimens from 1st set of experiments. The hatch distance is the first remarkable factor causing a lift for the overhanging geometry and it further enhances a separation after it reaches to a certain value of 1mm. The separation, despite the utilization of identical connection dimensions for all specimens in the 1st group, can be explained by inadequate strength of the support structures among themselves as a whole. Another indication of this situation can be seen on the influence of fragmentation factors to the results. Accordingly the specimens, which have fragmented islands comprising more cells, show less deformation. In the 2nd set of experiments, those include the investigation of connection dimensions; both the top length and Z offset value reductions influence the distortion results. However, the observed impact of Z offset value is inversely proportional with the top length. When the top length increases, the impact of Z offset value decreases. Besides, with the provision of lower values for top length dimensions, increased Z offset values reveal more deformation. One of the possible reasons that constitute this interesting result could be the use of different process parameters for part and support structures. But to examine the effect of different process parameters is beyond the scope of this paper.

After the dimensional inspection and test specimens were cut from the base plate, cross sections in two directions from the produced test parts were prepared for microstructural analysis (see Figure 3). The cross-sections were observed both in polished and etched conditions. During specimen preparation, some supports were detached from the part. The support structures built with higher hatch distance and fragmentation interval detached from the part significantly as also evident from Figure 4, where AA and BB cross-sections (as unpolished) for set 1 and set 2 tests are demonstrated. From the results of the second set of tests, the micrographs also show that top length with lower values for the tooth structures of the supports lead to weaker support attachments.

The density of produced parts was measured using the micrographs and the average porosity appears to be less than 0.1%. However, the cross-sectional micrographs in unpolished condition indicate some porosity close to the edges as evident from Figure 5. This result is probably due to the utilized scan strategy of using slightly different parameters for skin and edge areas leading to lower laser energy inputs. These parameters shall be optimized for less porosity which may have detrimental effect on the surface properties. As also stated in [33], since surface porosity is known to affect both the stress distribution and deformation of subsurface layers leading to subsurface crack formation and propagation, fully dense shell is especially important for applications requiring high wear resistance. Not only wear but also other surface properties such as thermal and electrical conductivity are highly dependent on the surface porosity.

Table 5 – Parts and results of the measurement

Measurement order

Parts of 1st set	Parts of 2nd set
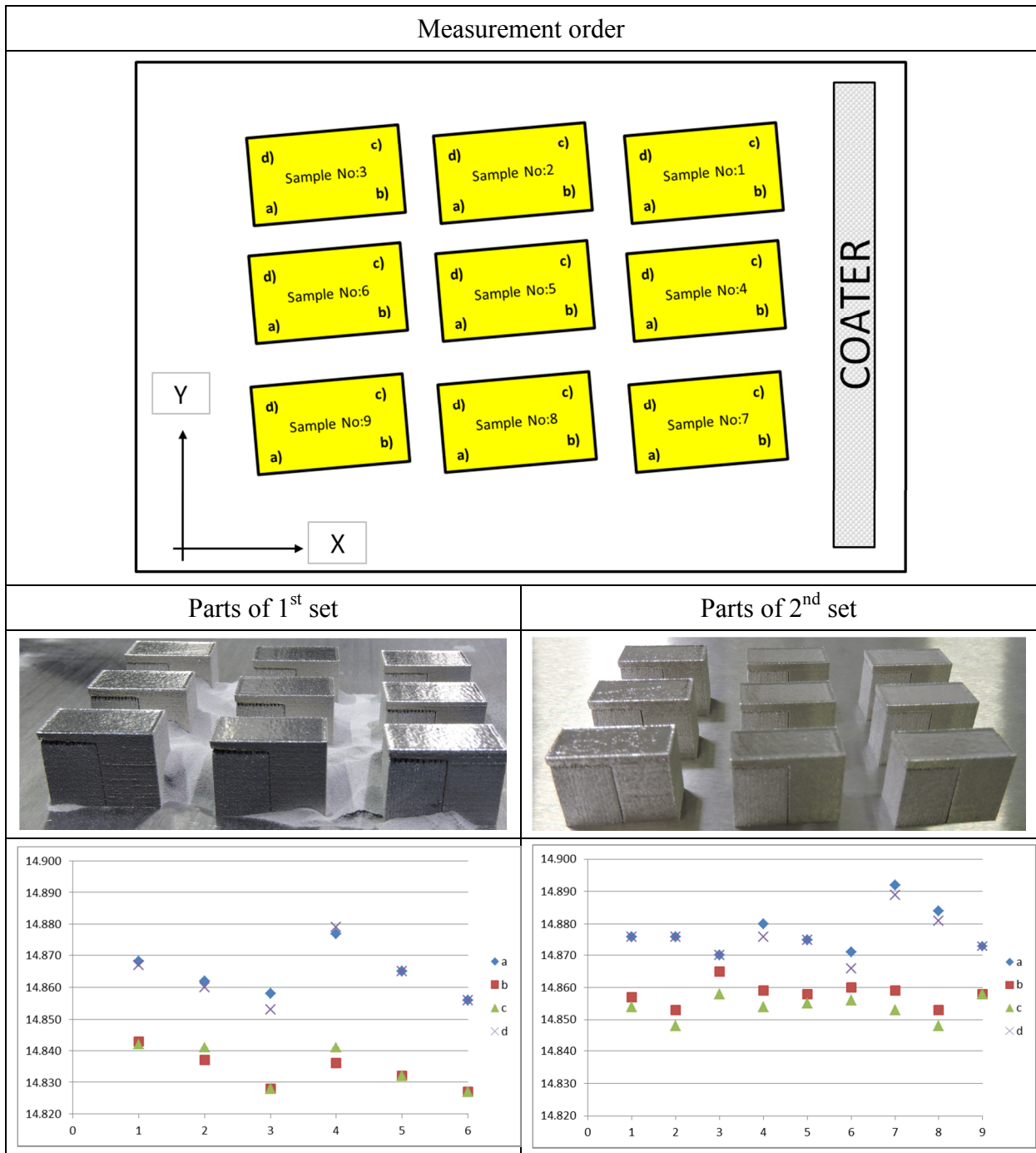
Regarding the microstructure of the produced test specimens, precipitates are observed densely close to the support structures. Figure 6 shows these precipitates for BB and AA cross-sections for the specimen b-9. In the study by Amato et al., these large intergranular precipitates are confirmed to be MoNb polyhedra having sizes ranging from 0.2 µm to 1 µm after SLM and HIP processes. However, in this study, no microstructural analysis method to determine the content of these precipitates has been carried out yet.
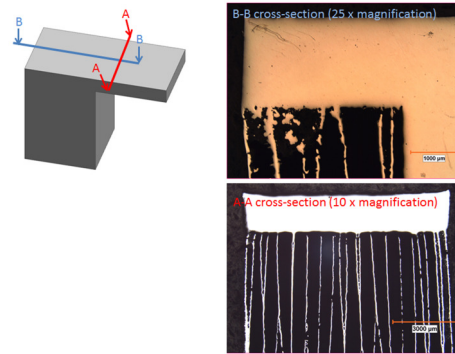
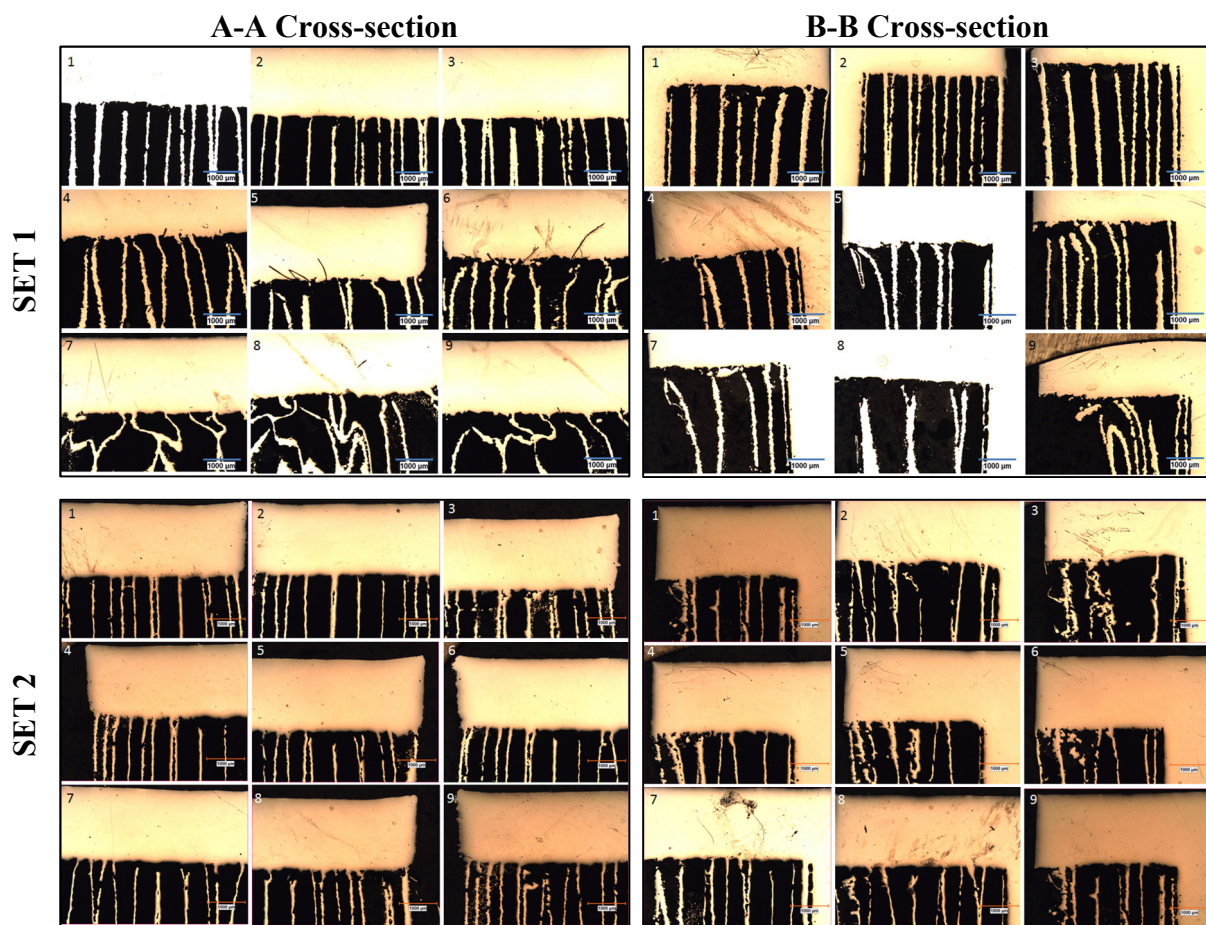Figure 3: The cross-sections prepared for microstructural analysis

Figure 4: The micrographs of test parts produced in Set 1 (above) and Set 2 (below)

The melt lines have been observed in laser fusion additive manufacturing processes with different materials [35-37]. The reason for observing these melt lines are attributed to the dark contrast distinguished these melt lines or bands arising by the enhanced precipitation of some phases [34, 38]. The melt lines are also observed in all specimens produced in this study. One of the specimen's (b-1) cross-sections are demonstrated in Figure 7 at two different magnification rates (200x and 500x). Regarding the IN625 material, these precipitates have been confirmed to be γ'' (bct-Ni$_3$Nb) in the literature. Moreover, it is shown with TEM analysis that the γ'' precipitates for SLM fabrication of IN625 occur as globular, nano particles in dense directional dislocation arrays while these γ'' nano particles range in size from ~30 nm–70 nm [38].
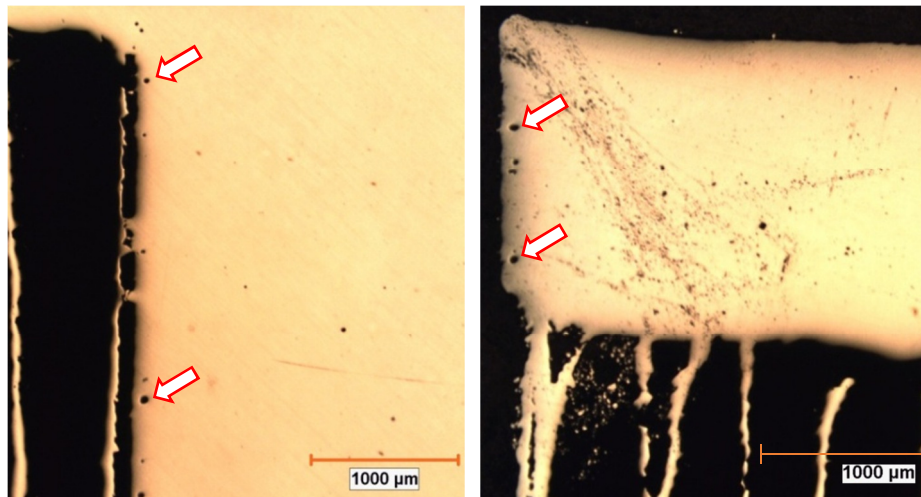
Figure 5: Porosity observed in the micrographs of test parts produced in b-5 for BB cross-section (left), b-7 for BB cross-section (right) (at 25x magnification)
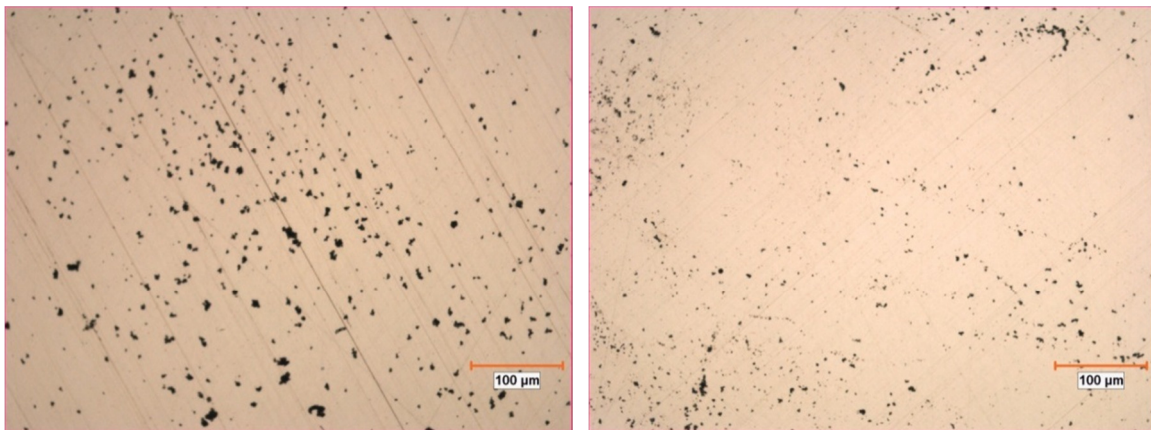

Figure 6: Precipitates in the two cross-sections of a specimen (b-9); BB cross-section (left) and AA cross-section (right)
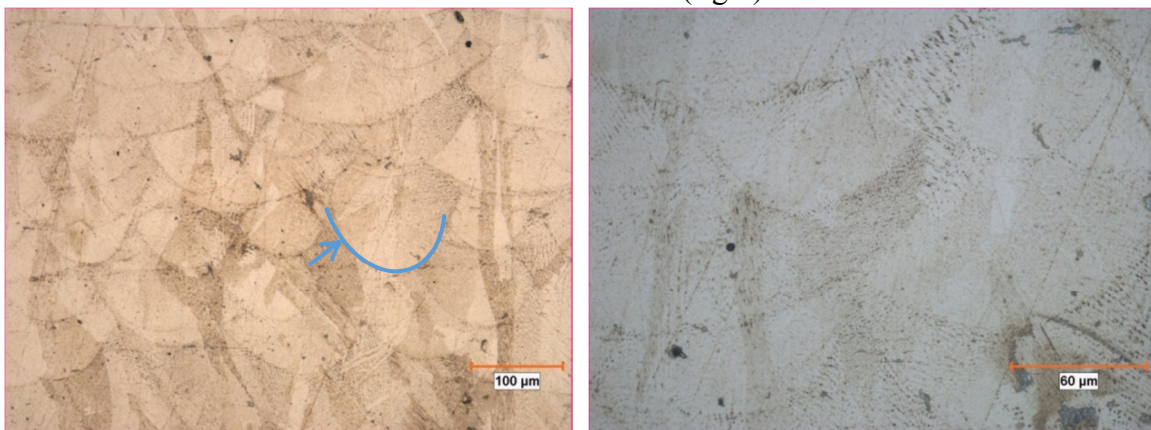

Figure 7: AA cross-section of a specimen (b-1): at 200x magnification (left) and at 500x magnification (right)

One of the reasons to conduct this study was to observe the grain formation at the connections of the support structures and the part and to understand if the geometrical features of a support structure have any influence on the grains. The micrographs of AA cross-sections of etched specimens are depicted in Figure 8 at 100x magnification. However, no clear trend

was observed for this effect. On the other hand, from some micrographs, it is evident that the self-detaching of the support structures from the part can lead to irregularities on the surface quality as well as some porosity formation (see Figure 9). Especially, for functional surfaces, special care shall be given for removing the supports to minimize the machining need.
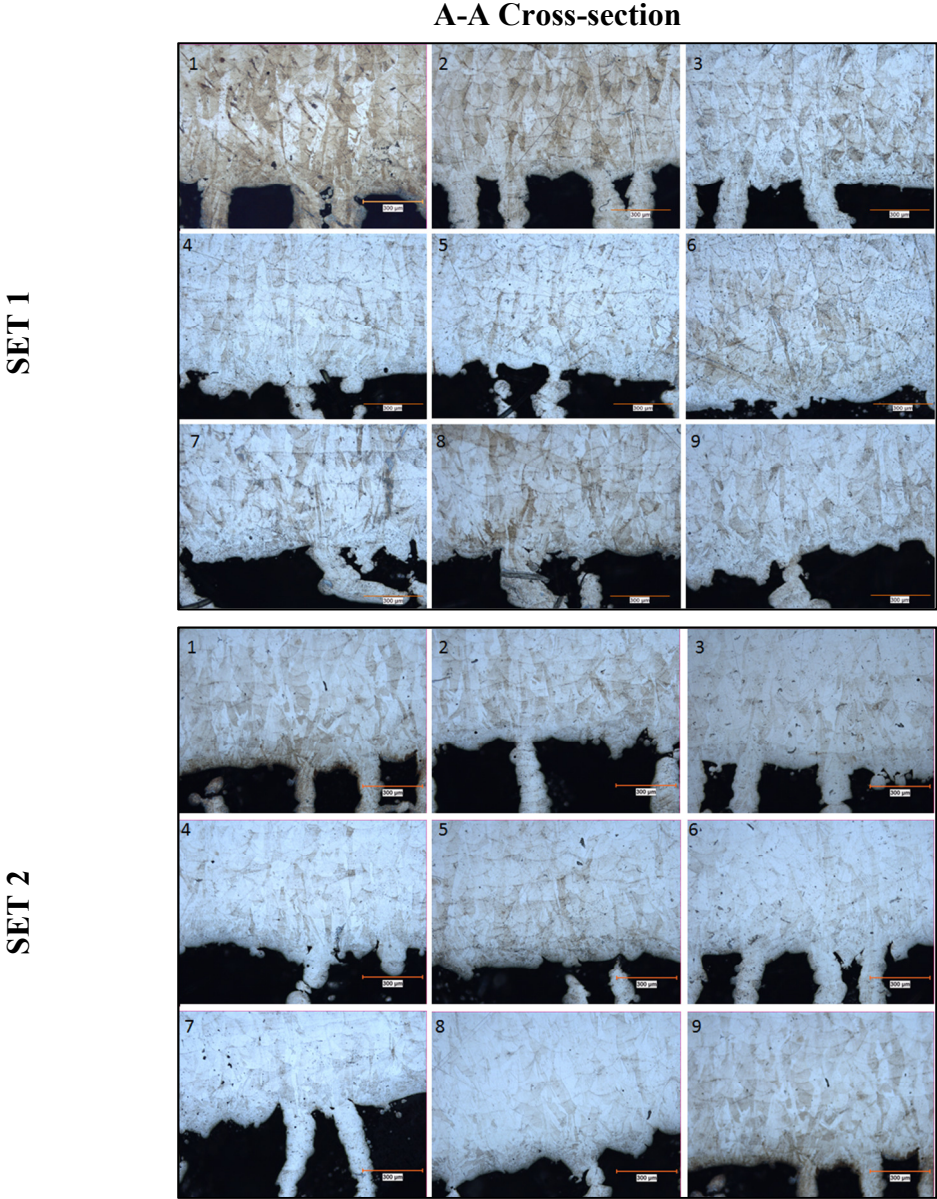
A-A Cross-section

Figure 8: The micrographs of test parts produced in Set 1 and Set 2: AA cross-sections in etched condition
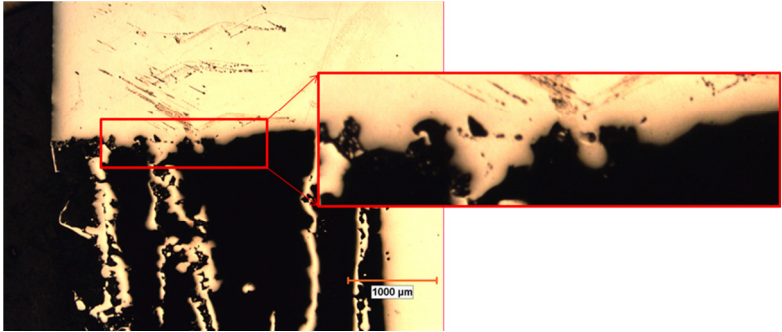

Figure 9: The micrograph of test b-3 – BB cross-section

Conclusions

In the presented study, support structures for DMLS processing of Inconel parts were investigated. A prismatic part with a parallel overhanging geometry was chosen in order to establish a need for support structures. A total of 18 samples were designed and manufactured in 2 sets to explore the effects of different design parameters on block type supports. Evaluated design parameters were hatch distance and fragmentation for the first set, tooth top length and Z offset for the second set. All samples were manufactured with constant process parameters to prevent the input of different variables rather than geometric criteria. After manufacturing, dimensional inspection was conducted by a height gage in order to see the part distortions. Results showed that, hatching parameters have greater influence on the support structures comparing to tooth parameters. Increased hatch distance enhances the distortion on the part, and even more it causes separation after a certain level. With respect to parallel overhanging geometries and block type support structures of IN625 alloy, conducted study have revealed that the application of lower hatch distance is useful in terms of maintaining less distortion and the best results among the examined range of values was achieved with 0.5mm hatch distance. After the dimensional inspection and test specimens were cut from the base plate, cross sections in two directions from the produced test parts were prepared for microstructural analysis. The cross-sections were observed both in polished and etched conditions. Separation problem was observed during specimen preparation in a consistent manner with the as built condition of the samples and dimensional inspections. The support structures built with higher hatch distance and fragmentation interval detached from the part easily. The micrographs also showed that top length with lower values for the tooth structures of the supports lead to weaker support attachments, but the adverse effect is lower than the hatch distance. Regarding the microstructure, precipitates were also observed densely close to the support structures. Furthermore, irregularities were detected on the part-support interface in the place of self-detaching support structures. The findings in the presented study demonstrate the effect of different parameters on block supports and provide guidance for designing these types of support structures.

References

1. ASTM F2792 – 12a Standard Terminology for Additive Manufacturing Technologies, DOI: 10.1520/F2792-12A.
2. VDI 3404 Additive Manufacturing: Basics, Definitions, Processes, May 2014.
3. Yasa, E., Demir, F., Akbulut, G., Cızıoğlu, N., & Pilatin, S. (2014) Benchmarking of Different Powder-Bed Metal Fusion Processes For Machine Selection In Additive Manufacturing. In Proceedings of Solid Freeform Fabrication Symposium, Austin, Texas.
4. Hague, R. (2006). Unlocking the design potential of rapid manufacturing. Rapid manufacturing: an industrial revolution for the digital age, John Wiley & Sons, Ltd.
5. Hussein, A., Hao, L., Yan, C., Everson, R., & Young, P. (2013). Advanced lattice support structures for metal additive manufacturing. Journal of Materials Processing Technology, 213(7), 1019-1026.
6. Mercelis, P. (2007) Control of Selective Laser Sintering and Selective Laser Melting Processes, Ph.D. Thesis, K.U.Leuven, Leuven, Belgium.
7. Craeghs, T., Clijsters, S., Yasa, E., Bechmann, F., Berumen, S., & Kruth, J. P. (2011). Determination of geometrical factors in layerwise laser melting using optical process monitoring. Optics and Lasers in Engineering, 49(12), 1440-1446.
8. Cheng, B., & Chou, K. (2014) Thermal Stresses Associated with Part Overhang Geometry in Electron Beam Additive Manufacturing: Process Parameter Effects. In Solid Freeform Fabrication Symposium, Austin, Texas.
9. Moroni, G., Syam, W. P., & Petrò, S. (2015). Functionality-based part orientation for additive manufacturing. In Proceedings of 25th CIRP Design Conference, Haifa, Israel.
10. Wang, D., Yang, Y., Yi, Z., & Su, X. (2013). Research on the fabricating quality optimization of the overhanging surface in SLM process. The International Journal of Advanced Manufacturing Technology, 65(9-12), 1471-1484.
11. Craeghs, T. (2012), A monitoring system for online control of Selective Laser Melting, Ph.D. Thesis, K.U.Leuven, Leuven, Belgium.
12. Thomas, D. (2009). The development of design rules for selective laser melting, Doctoral dissertation, University of Wales, Cardiff, UK.
13. Wegner, A., & Witt, Gerd., (2012). Konstruktionsregeln für das Laser-Sintern, Zeitschrift Kunststofftechnik, Vol. 8, No. 3, pp. 253-277.
14. www.solidconcepts.com/resources/design-guidelines/
15. Allen, S., & Dutta, D. (1994, September). On the computation of part orientation using support structures in layered manufacturing. In Proceedings of Solid Freeform Fabrication Symposium, University of Texas at Austin, Austin, TX, June (pp. 259-269).
16. Cloots, M., Spierings, A. B., & Wegener, K. (2013). Assessing new support minimizing strategies for the additive manufacturing technology SLM. In Solid Freeform Fabrication Symposium, Austin, Texas.
17. Gibson, I., Rosen, D. W., & Stucker, B. (2010). Additive manufacturing technologies. New York: Springer.
18. Chalasani, K., Jones, L., & Roscoe, L. (1995, August). Support generation for fused deposition modeling. In Proceedings of Solid Freeform Fabrication Symposium, Austin, Texas.
19. software.materialise.com/magics-sg-module
20. www.netfabb.com/structure.php

21. www.fabbify.com/en/links-additive-manufacturing-software.html
22. www.smart3d.net/supportgenerator
23. Majhi, J., Janardan, R., Schwerdt, J., Smid, M., & Gupta, P. (1999). Minimizing support structures and trapped area in two-dimensional layered manufacturing. Computational Geometry, 12(3), 241-267.
24. Hussein, A., Yan, C., Everson, R., & Hao, L. (2011). Preliminary investigation on cellular support structures using SLM process. Innovative Developments in Virtual and Physical Prototyping. Taylor & Francis Group, London, 609-612.
25. Krol, T. A., Zäh, Ö.F., Schlip, J., & Seidel, C. (2011) Computational Efficient Design Structures and Material Modeling for Metal Based Additive Manufacturing. ANSYS Conference & 29th CADFEM Users' Meeting, Stuttgart.
26. Krol, T. A., Zäh, M. F., & Seidel, C. (2012). Optimization of supports in metal-based additive manufacturing by means of finite element models. In Solid Freeform Fabrication Symposium
27. Bo, Q., Lichao, Z., Yusheng, S., & Guocheng, L. (2012). Support fast generation algorithm Based on discrete-marking in rapid prototyping. In Affective Computing and Intelligent Interaction (pp. 683-695). Springer Berlin Heidelberg.
28. Strano, G., Hao, L., Everson, R. M., & Evans, K. E. (2013). A new approach to the design and optimisation of support structures in additive manufacturing. The International Journal of Advanced Manufacturing Technology, 66(9-12), 1247-1254.
29. Krol, T. A., Seidel, C., Schilp, J., Hofmann, M., Gan, W., & Zaeh, M. F. (2013). Verification of structural simulation results of metal-based additive manufacturing by means of neutron diffraction. Physics Procedia, 41, 849-857.
30. Calignano, F. (2014). Design optimization of supports for overhanging structures in aluminum and titanium alloys by selective laser melting. Materials & Design, 64, 203-213.
31. Special Metals, Inconel ® alloy 625 material data sheet.
32. EOS material datasheet for Nickel Alloy IN625.
33. Yasa, E. (2011). Manufacturing by Combining Selective Laser Melting and Selective Laser Erosion / Laser Re-Melting, Ph.D. Thesis, K.U.Leuven, Leuven, Belgium.
34. Amato, K.N., Hernandez, J., Murr, L.E., Martinez, E., Gaytan, S.M., Shindo, P.W. (2012), Comparison of Microstructures and Properties for a Ni-Base superalloy (Alloy 625) fabricated by electron and laser beam melting. Journal of Materials Science Research, Vol. 1, No 2, pp.3-41.
35. Kruth, J.-P., Badrossamay, M., Yasa, E., Deckers, J., Thijs, L., Van Humbeeck, J. (2010). Part and material properties in selective laser melting of metals. In Proc. of the 16th International Symposium on Electromachining (ISEM XVI) edition:16, Shanghai, China, 19-23 April 2010.
36. Thijs, L. (2009). Invloed van het selectief laser smelten op de microstructuur van titaanlegeringen, Master Thesis, K.U.Leuven, Leuven, Belgium.
37. Manfredi, D.,Calignano, F., Krishnan, M., Canali,R.,Ambrosio, E.P., Atzeni, E. (2013), Materials, 6, 856-869; doi:10.3390/ma6030856.
38. Murr, L.E., Martinez, E., Amato, K.N., Gaytan, S.M., Hernandez, J., Ramirez, D.A., Shindo, P.W., Medina, F., Wicker, R.B. (2012). Fabrication of Metal and Alloy Components by Additive Manufacturing: Examples of 3D Materials Science, Journal of Materials and Research Technology, pp.42-54.